Supporting Information

Optimal electrolyte pH for efficient quinone-based aqueous redox flow battery and solar cell integration

Joao Otavio Mendes,[1] *Rasmus Svejstrup Nielsen,*[1] *Tobias Høyrup Hemmingsen,*[1] *Thomas K. Rønne-Nielsen,*[2] *Susanne Mossin,*[2] *Ole Hansen*[3] *and Peter Christian Kjærgaard Vesborg*[1*]

[1] SurfCat, DTU Physics, Technical University of Denmark, Kongens Lyngby 2800, Denmark.

[2] DTU Chemistry, Technical University of Denmark, Kongens Lyngby 2800, Denmark.

[3] National Centre for Nano Fabrication and Characterisation (DTU Nanolab), Technical University of Denmark, 2800 Kongens Lyngby, Denmark.

* peter.vesborg@fysik.dtu.dk

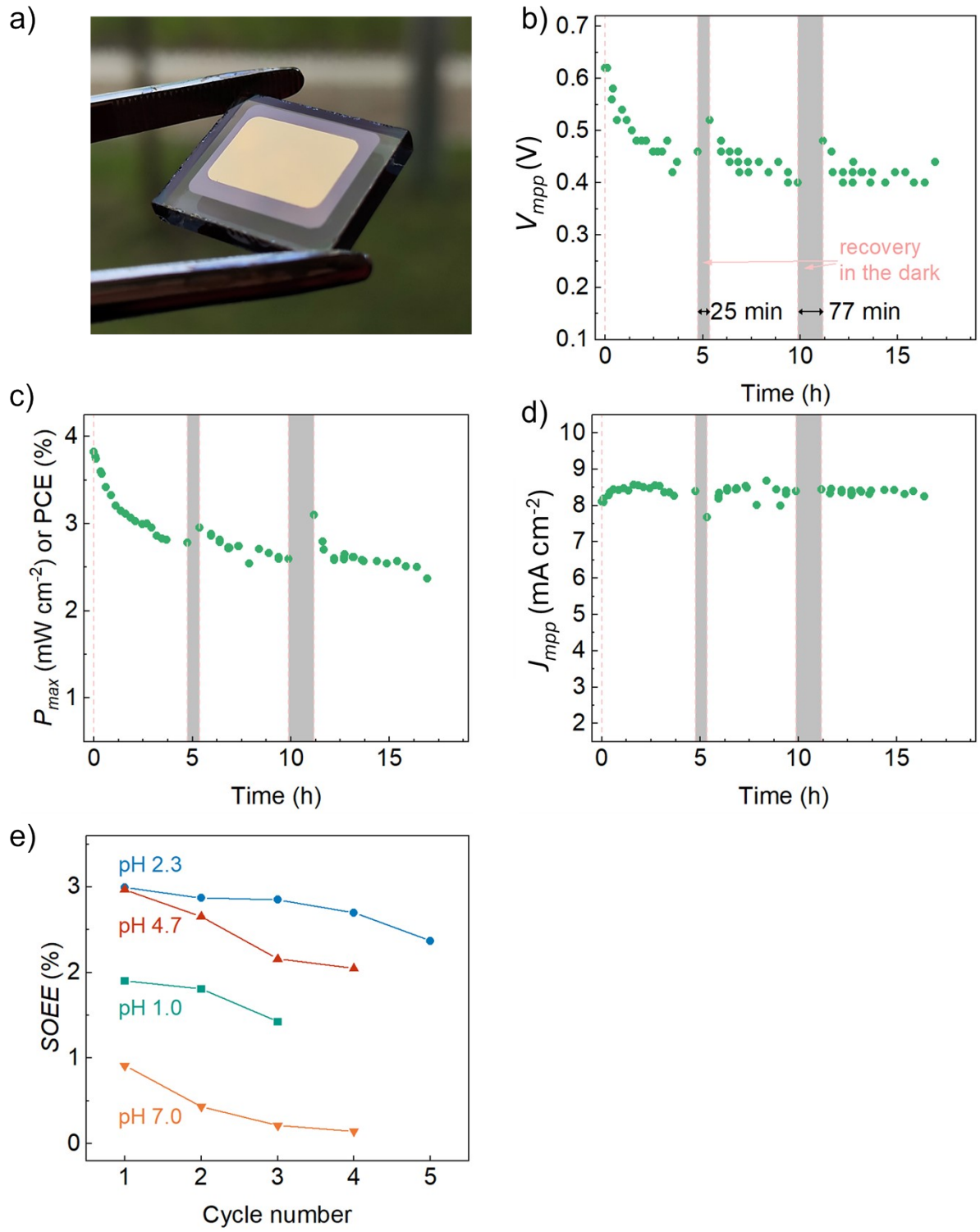

Figure S1 a) Back side of a Se solar cell (FTO/ZnMgO/Se/MoO_x/Au), the gold rectangle is 11 x 8 mm (back contact). Data extracted from *JV* curves taken for a cell kept under constant light exposure (1 sun, AM1.5G), b) V_{mpp}, c) P_{max} and d) J_{mpp}. The dark bars indicate recovery time in the dark. e) System stability (extra cycles) for a SRFB with 2,7-AQDS anolyte buffered at different pH values. The decrease in *SOEE* is attributed to the lower V_{mpp} over prolonged light exposure. We limited cycling within working hours for added safety during the continuous operation of our solar simulator. Thus, due to this time limitation, it was not possible to realise 5 full charge/discharge cycles for all the pHs investigated here.

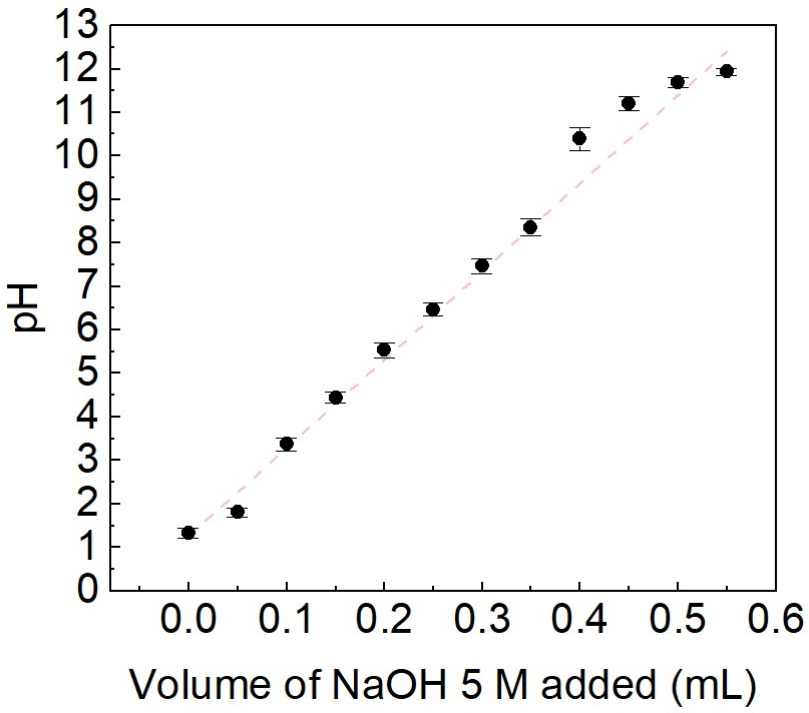

Figure S2 pH calibration for 5 ml of buffer solution prepared by mixing H_3PO_4 (pKa_1 = 2.15, pKa_2 = 7.2 and pka_3 = 12.35), CH_3COOH (pKa = 4.76) and Tris·HCl (pKa = 8.1) to a final concentration of 0.1 M for each acid.

Equation S1: Relationship between $E_{1/2}$ and proton concentration[1]

$$E_{1/2} = E^0 + 0.0296log\left(1 + \frac{[H^+]}{K_{a6}} + \frac{[H^+]^2}{K_{a3}K_{a6}}\right)$$

Equation S2: Nernst equations and pH[2]

$$AQDS^{-2} + 2e^- + nH^+ \rightarrow (AQDSH_n)^{n-4}$$

$$E = E^0 - \frac{RT}{zF}ln\frac{1}{[H^+]^n} = E^0 - \frac{0.059n}{z}pH$$

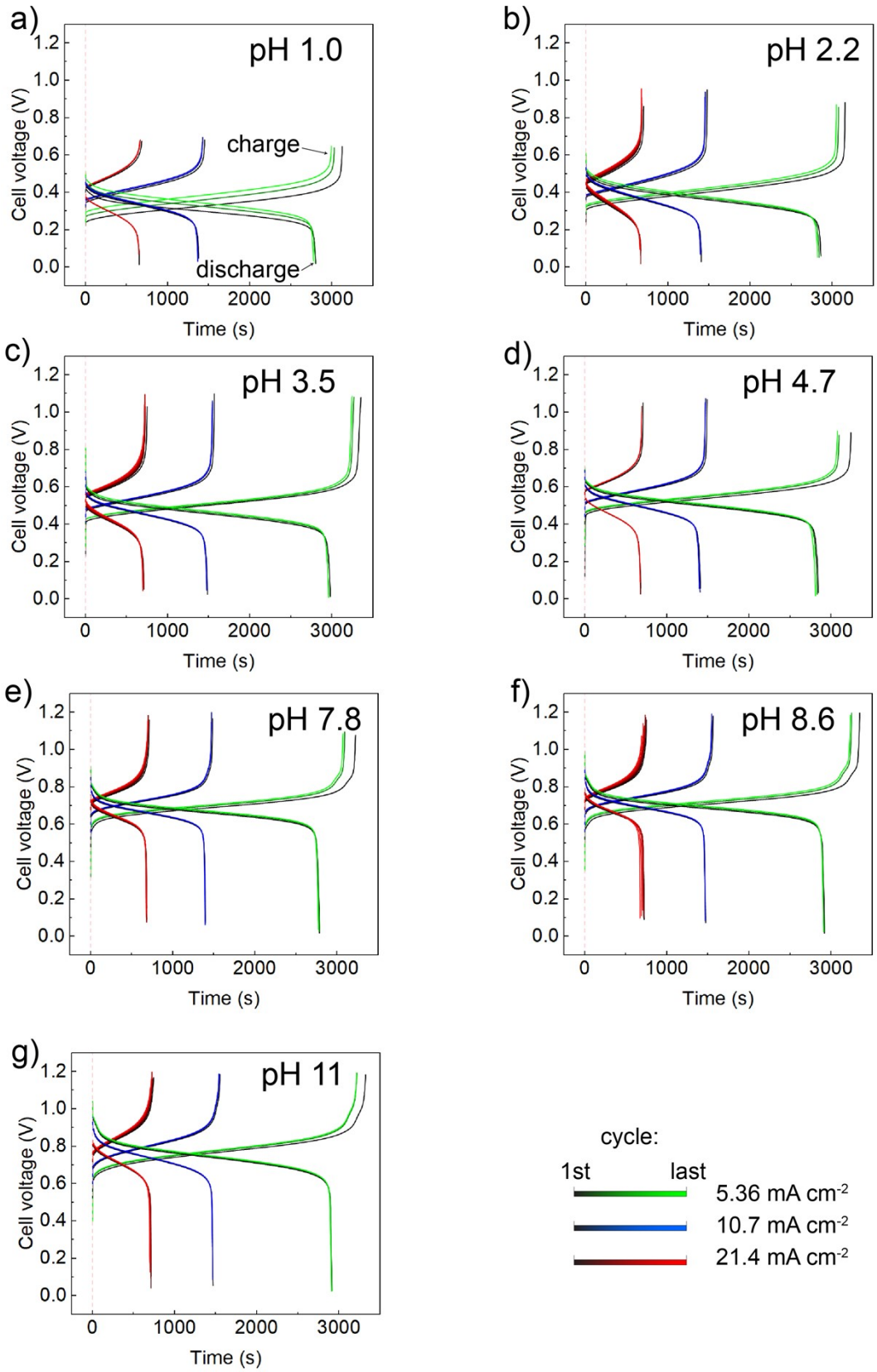

Figure S3 Charge and discharge curves at 5.36, 10.7 and 21.4 mA cm^{-2} for 2,7-AQDS (10 mM)-ferrocyanide (40 mM) redox flow battery with anolyte buffered at pH a) 1.1, b) 2.2, c) 3.5, d) 4.7, e) 7.8, f) 8.6 and g) 11.

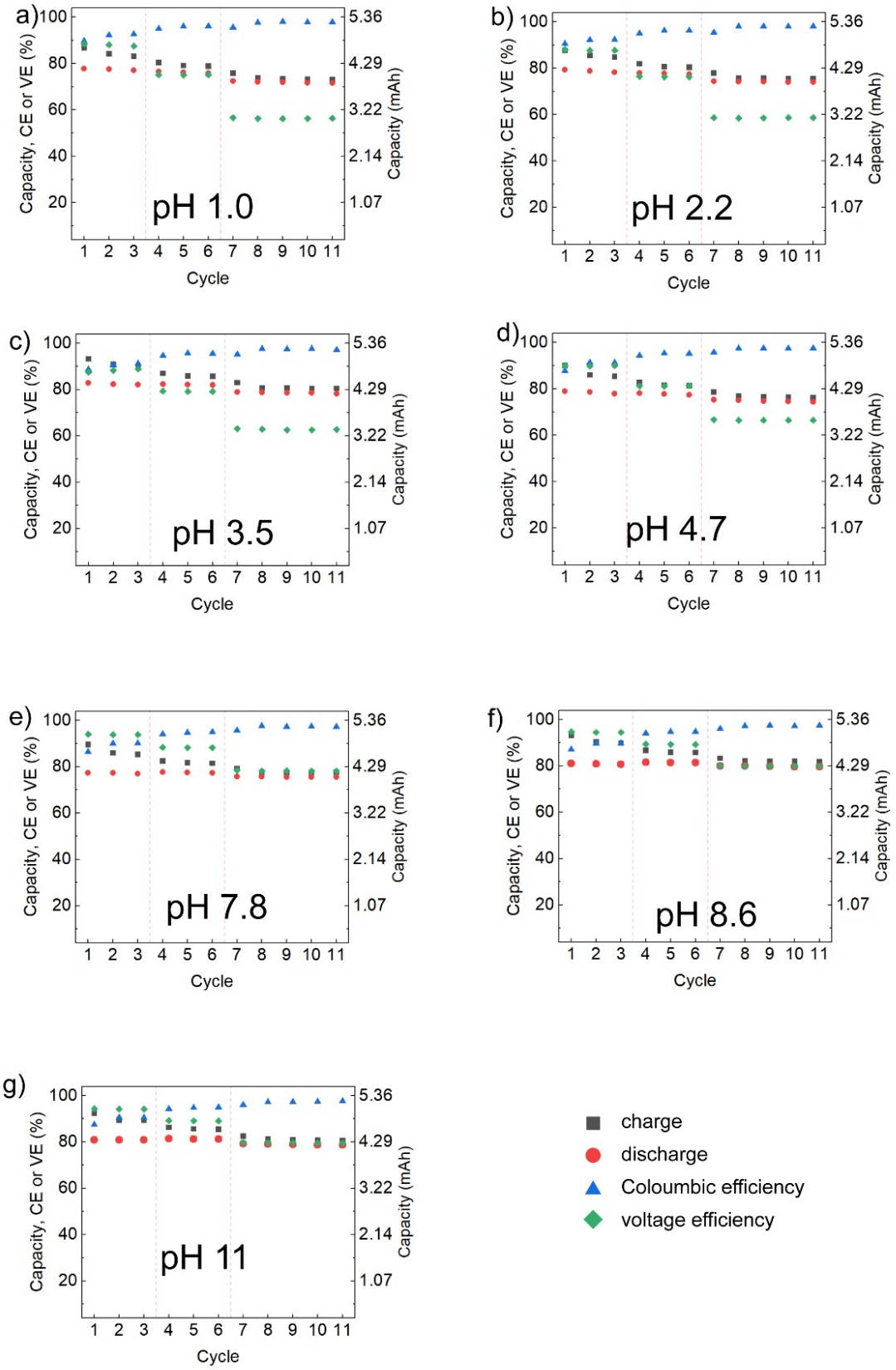

Figure S4 Charge and discharge capacities, Coulombic efficiency and voltage efficiency at 5.36, 10.7 and 21.4 mA cm^{-2} for 2,7-AQDS (10 mM)-ferrocyanide (40 mM) redox flow battery with anolyte buffered at pH a) 1.1, b) 2.2, c) 3.5, d) 4.7, e) 7.8, f) 8.6 and g) 11.

Calculated *SOEE* and voltage matching

The solar-to-output electricity (*SOEE*) of a solar redox flow battery (SRFB) can be estimated over a range of electrochemical cell potentials (E_{cell}) using simulated Nernstian charging curves. The calculated *SOEE* is then obtained by matching the experimental *JV* curve for the solar cell with simulated charging curves with varying E^{0}_{cell}. The full derivation of the equations and theory can be found elsewhere in the literature.[3], [4] In short, the Nernstian charging curves were generated by using the equation:

$$E_{cell} = E^{0}_{cell} - \frac{RT}{F}\left(\frac{1}{n_{catholyte}} + \frac{1}{n_{anolyte}}\right) ln\left[\frac{1 - SOC}{SOC}\right]^2 + \eta$$

Where R is the gas constant, T is the temperature in K, F is Faraday's constant, n is the number of electrons transferred for each mol of active species at the catholyte or anolyte and *SOC* is the state of charge of the cell. The overpotential (η) was considered negligible.

The instantaneous solar-to-output electricity efficiency ($SOEE_{ins}$), that represents the efficiency at any given *SOC* is calculated by:

$$SOEE_{ins} = \frac{P_{electrical,discharge}}{P_{illumination}} = \frac{I_{operating} V_{operating}}{SA} CE \cdot VE$$

where $P_{electrical,discharge}$ is the electrical power during discharge of the battery, $P_{illumination}$ is the power provided by the simulated sunlight, $I_{operating}$ is the photocurrent provided by the solar cell at a corresponding operating potential ($E_{cell} = V_{operating}$), S is the solar irradiance and A is the active area of the solar cell, CE and VE are the Coulombic- and voltage efficiencies. The energy efficiency ($EE = CE \times VE$) was set at 85% to estimate *SOEE*. The *SOEE* is then obtained by discrete integration of $SOEE_{ins}$ over the relevant SOC interval (1 to 99% for a full charge):

$$SOEE = \frac{\sum_{i-m}^{n} SOEE_{ins}}{n - m + 1}$$

By plotting the *SOEE* as a function of E_{cell} we can determine the most adequate cell potential for integration with a specific solar cell.

Experimental *SOEE*

The experimental *SOEE* of the semi-integrated system was obtained using the current and voltage measured during solar charge and discharge of the electrochemical cell. $SOEE_{ins}$ and *SOEE* were obtained in a similar manner as explained in the previous section:

$$SOEE_{ins} = \frac{P_{electrical,discharge}}{P_{illumination}} = \frac{I_{operating} V_{operating}}{SA} CE \cdot VE$$

where $I_{operating}$ and $V_{operating}$ are now measured by the current meter and potentiostat, respectively, during the solar charge. S is 100 mW cm^{-2}, A is the area of the gold contact 0.8cm^2, and CE and VE are:

$$CE = \frac{Q_{discharge}}{Q_{charge}} = \frac{\int I_{discharge} dt}{\int I_{operating} dt}$$

$$VE = \frac{\overline{V}_{discharge}}{\overline{V}_{charge}} = \frac{\int V_{discharge} d^t / \int dt}{\int V_{operating} d^t / \int dt}$$

Finally, the experimental *SOEE* is obtained from:

$$SOEE = \frac{E_{Electrical,discharge}}{E_{illumination}} = \frac{\int I_{discharge} V_{discharge} dt}{\int SA dt}$$

Where $E_{Electrical,discharge}$ and $E_{illumination}$ are the experimental energies of battery discharge and illumination, respectively.

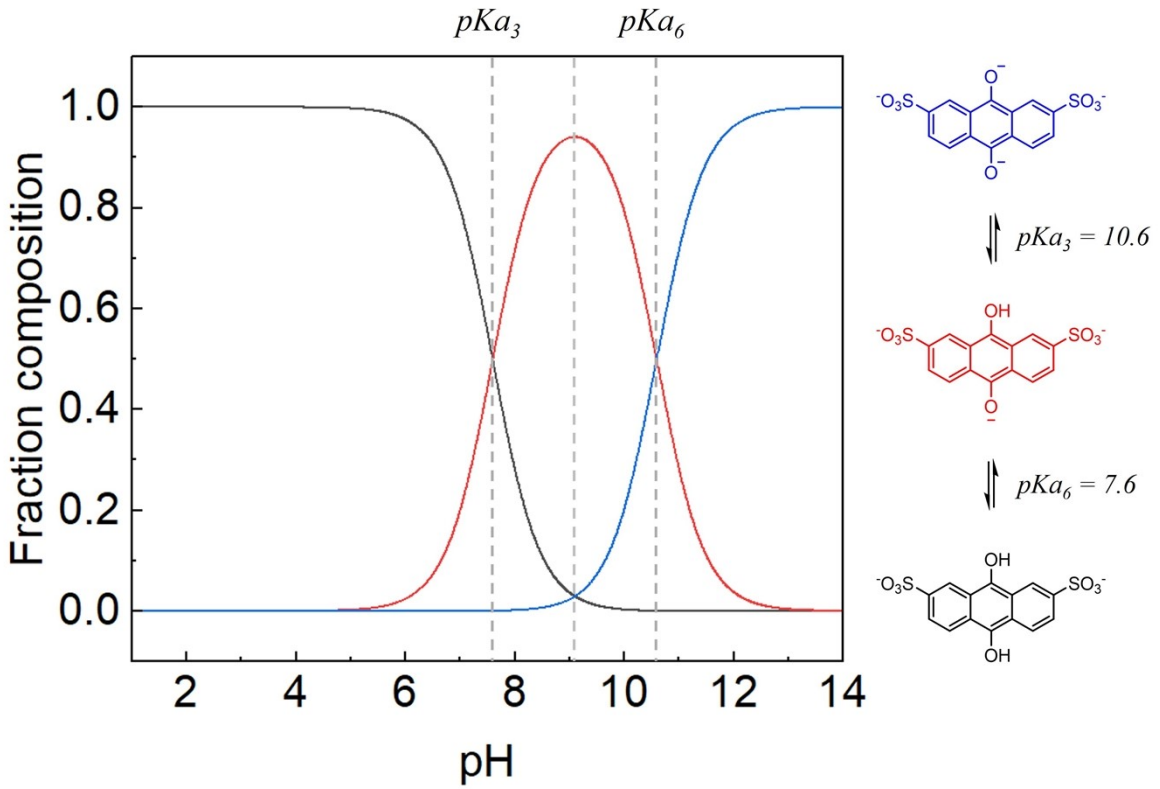

Figure S5 Fraction composition of completely reduced (charged) 2,7-AQDS.

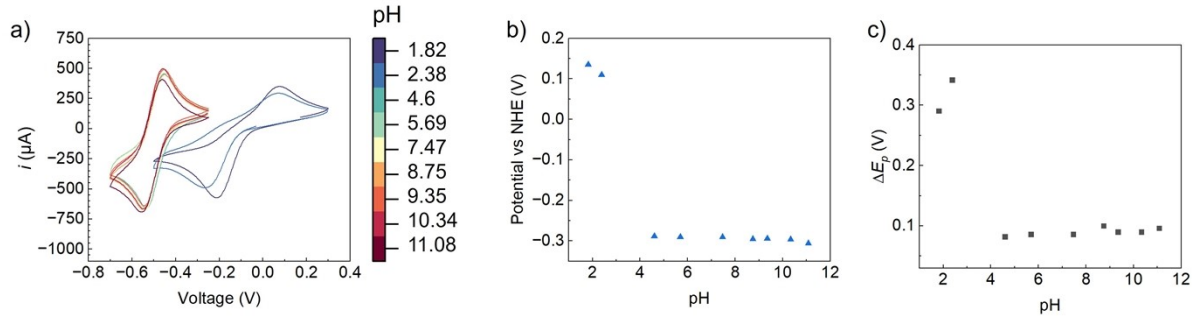

Figure S6 Unbuffered 10mM 2,7-AQDS solutions a) CV curves, b) $E_{1/2}$ and c) peak separation (ΔE_p).

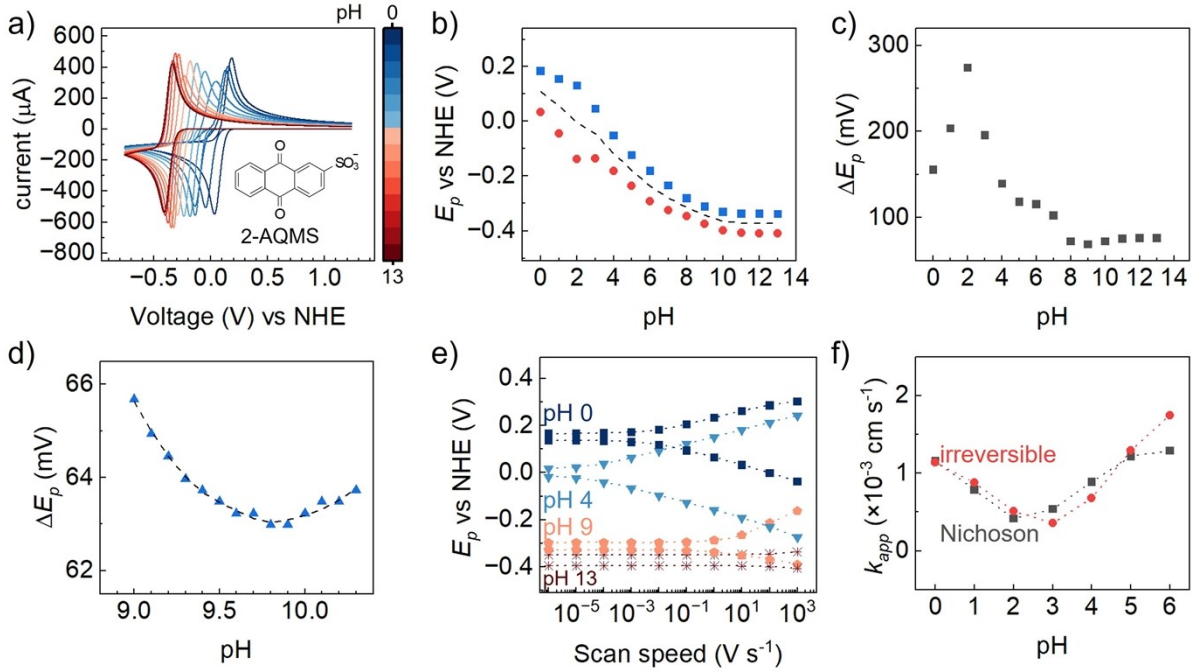

Figure S7 Simulated kinetic data for a buffered 2-AQMS anolyte a) CV curves, b) peak position (E_p), c) and d) peak separation (ΔE_p), e) Laviron curves for selected pHs, and f) apparent kinetic constant (k_{app}) extracted from Laviron curves using equation for totally irreversible systems and Nicholson methods. Simulation parameters are given in the **Table S2**.

Table S1 Redox flow battery parameters voltage efficiency (*VE*), Coulombic efficiency (*CE*), energy efficiency (*EE*) and average voltage drop on the round trip (E_{drop})

VE	$\frac{\overline{V}_{discharge}}{\overline{V}_{charge}} = \frac{\int V_{discharge} d^t / \int dt}{\int V_{charge} d^t / \int dt}$
CE	$\frac{Q_{discharge}}{Q_{charge}} = \frac{\int I_{discharge} dt}{\int I_{operating} dt}$
EE	$CE \times VE$
E_{drop}	$\overline{V}_{charge} - \overline{V}_{discharge} = \int V_{charge} dt - \int V_{discharge} dt$

Table S2 Simulation parameters for 2,7-AQDS and 2-AQMS

	2,7-AQDS	**2-AQMS**
Diagram of squares	$AQ \overset{E_1}{\rightleftharpoons} AQ^{\bullet-} \overset{E_2}{\rightleftharpoons} AQ^{2-}$ $pKa_1 \downarrow\uparrow \quad pKa_2 \downarrow\uparrow \quad pKa_3 \downarrow\uparrow$ $AQH^{+} \overset{E_3}{\rightleftharpoons} AQH^{\bullet} \overset{E_4}{\rightleftharpoons} AQH^{-}$ $pKa_4 \downarrow\uparrow \quad pKa_5 \downarrow\uparrow \quad pKa_6 \downarrow\uparrow$ $AQH_2^{2+} \overset{E_5}{\rightleftharpoons} AQH_2^{\bullet+} \overset{E_6}{\rightleftharpoons} AQH_2$	
$C_{initial}$ (mol/L)[1]	0.01	0.01
$R_{uncompensated}$ (ohm)	20 (or 0 for speed dependent simulations)	
D_0 (cm^2 s^{-1})[2] [5]	2×10^{-6}	3×10^{-6}
Reaction pathway [5]	CECE (pH 0 - 3) ECEC (pH 4 - 7) EECC (pH 8 - 13)	CECE (pH 0 - 2) ECEC (pH 3 - 6) EECC (pH 7 - 13)
Electrochemical step (E)	$A + e^- \rightleftharpoons B$	
E_n(V vs NHE)[3], k^0 (cm^2 s^{-1}) [5], [6]	$E_1 = -0.28799$, $k^0 = 0.025$ $E_2 = -0.32399$, $k^0 = 0.1$ $E_3 = 0.207$, $k^0 = 1$ $E_4 = 0.10741$, $k^0 = 10$ $E_6 = 0.21181$, $k^0 = 0.0189$	$E_1 = -0.3651$, $k^0 = 10$ $E_2 = -0.38001$, $k^0 = 0.38067$ $E_3 = -0.1585$, $k^0 = 10$ $E_4 = 0.01419$, $k^0 = 10$ $E_6 = 0.27913$, $k^0 = 10$
α	0.5	
Chemical step (C)	(protonated) $B \rightleftharpoons A$ (unprotonated)	
pK_{a_n}[5], [6]	$pK_{a_1} = 0$ $pK_{a_2} = 3.2$ $pK_{a_3} = 10.6$ $pK_{a_4} = 4.8$ $pK_{a_6} = 7.6$	$pK_{a_1} = 0.84$ $pK_{a_2} = 4.3$ $pK_{a_3} = 11$ $pK_{a_4} = 3.12$ $pK_{a_6} = 7.6$
$k_{f(max)}$	Arbitrary	
k_{f4}	$k_{f(max)}[H^+]$	
k_b	k_f / K_{eq}	
K_{eq}	$K_a / [H^+]$	

[1] Initial concentration of completely oxidized (not protonated) molecule.
[2] Same for all species
[3] Converted from SCE with a factor of +0.241 V from reference [5] and [6]
[4] 1st order with proton concentration, $k_{f(max)}$ is adjusted so that $k_f \leq 10^{10}$.

$[H^+]$	from 10^0 to 10^{-13}

Apparent kinetic constant (k_{app})

The apparent kinetic constants (k_{app}) were determined using the methods for totally irreversible and quasireversible (Nicholson) systems.

Assuming a totally irreversible system, the following equation was applied (v > 1 V s^{-1}):[7]

$$E_p = E_{1/2} + \frac{1}{\alpha nf}\left(-0.78 + \ln\frac{k_{app}}{\sqrt{\alpha nf v D_o}}\right), f = \frac{F}{RT}$$

The slope of the plot of E_p vs ln v is proportional to α, while the intercept gives E_{00}: [8]

$$E_p = a\ln v + E_{00}, a = \frac{1}{2\alpha nf}$$

The equation for k_{app} then becomes:

$$k_{app} = \exp\left(\alpha nf\left(E_{00} - E_{1/2}\right) + 0.78 + \ln\sqrt{\alpha nf D_0}\right)$$

with $D_0 = 2\times10^{-6}$ cm^2 s^{-1} and $n = 2$:

Assuming a quasireversible system, the Nicholson method was used by applying the following equation (v > 1 mV s^{-1}): [9]

$$\Psi = k_{app}\left(\frac{\pi D_0 nF}{RT}\right)^{-\frac{1}{2}} v^{-\frac{1}{2}}$$

The slope of a plot of Ψ vs $v^{-\frac{1}{2}}$ was used to determine k_{app} with $D_0 = 2\times10^{-6}$ cm^2 s^{-1} and $n = 2$. The value of Ψ was determined using the empirical equation:[10]

$$\Psi = \frac{-0.6288 + 0.0021n\Delta E_p}{1 + 0.017n\Delta E_p}$$

[1] M. Quan, D. Sanchez, M. F. Wasylkiw, and D. K. Smith, "Voltammetry of quinones in unbuffered aqueous solution: Reassessing the roles of proton transfer and hydrogen bonding in the aqueous electrochemistry of quinones," *J Am Chem Soc*, vol. 129, no. 42, pp. 12847–12856, 2007, doi: 10.1021/ja0743083.

[2] B. Hu, J. Luo, M. Hu, B. Yuan, and T. L. Liu, "A pH-Neutral, Metal-Free Aqueous Organic Redox Flow Battery Employing an Ammonium Anthraquinone Anolyte," *Angewandte Chemie - International Edition*, vol. 58, no. 46, pp. 16629–16636, 2019, doi: 10.1002/anie.201907934.

[3] W. Li *et al.*, "High-performance solar flow battery powered by a perovskite/silicon tandem solar cell," *Nat Mater*, vol. 19, no. 12, pp. 1326–1331, 2020, doi: 10.1038/s41563-020-0720-x.

[4] W. Li and S. Jin, "Design Principles and Developments of Integrated Solar Flow Batteries," *Acc Chem Res*, vol. 53, no. 11, pp. 2611–2621, 2020, doi: 10.1021/acs.accounts.0c00373.

[5] C. Batchelor-McAuley, Q. Li, S. M. Dapin, and R. G. Compton, "Voltammetric characterization of DNA intercalators across the full pH range: Anthraquinone-2,6-disulfonate and anthraquinone-2-sulfonate," *Journal of Physical Chemistry B*, vol. 114, no. 11, pp. 4094–4100, 2010, doi: 10.1021/jp1008187.

[6] C. Wiberg, T. J. Carney, F. Brushett, E. Ahlberg, and E. Wang, "Dimerization of 9,10-anthraquinone-2,7-Disulfonic acid (AQDS)," *Electrochim Acta*, vol. 317, pp. 478–485, 2019, doi: 10.1016/j.electacta.2019.05.134.

[7] A. J. Bard and L. R. Faulkner, *Electrochemical Methods Fundamentals and Applications (2nd edition)*, vol. 48, no. 2. 2001.

[8] Biologic, "CV Sim: Simulation of the simple redox reaction (E) – Part I: The effect of scan rate Kinetics – Application Note 41-1," 2022.

[9] R. S. Nicholson, “Theory and Application of Cyclic Voltammetry for Measurement of Electrode Reaction Kinetics,” *Anal Chem*, vol. 37, no. 11, pp. 1351–1355, 1965, doi: 10.1021/ac60230a016.

[10] I. Lavagnini, R. Antiochia, and F. Magno, “An extended method for the practical evaluation of the standard rate constant from cyclic voltammetric data,” *Electroanalysis*, vol. 16, no. 6, pp. 505–506, 2004, doi: 10.1002/elan.200302851.